Experimental validation of multi-sensor data fusion model for railway wheel defect identification

Alemi, Alireza; Pang, Yusong; Lodewijks, Gabri

Publication date
2018

Document Version
Final published version

Published in
Proceedings of the 4th European Conference of the Prognostics and Health Management Society (PHM Europe 2018)

Citation (APA)
Alemi, A., Pang, Y., & Lodewijks, G. (2018). Experimental validation of multi-sensor data fusion model for railway wheel defect identification. In C. S. Kulkarni, & T. Tinga (Eds.), *Proceedings of the 4th European Conference of the Prognostics and Health Management Society (PHM Europe 2018)* PHM Society.

Experimental Validation of Multi-Sensor Data Fusion Model for Railway Wheel Defect Identification

Alireza Alemi[1], Yusong Pang[2], and Gabriel Lodewijks[3]

[1,2] *Faculty of Mechanical, Maritime and Material Engineering (3mE), Delft University of Technology, Delft, 2628 CD, The Netherlands*
A.Alemi@tudelft.nl
Y.Pang@tudelft.nl

[3] *School of Aviation, University of New South Wales, Sydney, NSW 2052, Australia*
g.lodewijks@unsw.edu.au

ABSTRACT

Wheel defects are detrimental for railway train and track components and should be detected and identified as early as possible. Wheel Impact Load Detector (WILD) is a commercial condition monitoring system used for detecting the defective wheels. This system usually measures the rail strain at different points by multiple sensors. WILD converts the measured strains to the force and uses the peak force, dynamic force, and ratio of the peak force to the static force to estimate the condition of the in-service wheels. These methods are useful for detecting the severe defects contributing to the contact force to the extent that exceed a predetermined threshold. Therefore, in the prior research a fusion method has been developed to reconstruct a new informative pattern from the data collected by the multiple sensors. The reconstructed pattern provides a comprehensive description of the wheel condition. This paper validates the fusion method using a set of lab tests to investigate the applicability of the proposed method. For this purpose, a test rig has been built consisting of a circular rail, a rotating arm, and a wheel. Six strain sensors have been installed under the rail in the symmetric locations over the rail circle with 60 degree intervals. The fusion method used to reconstruct a signal from the bending strain signals measured by the multiple sensors. Different wheel defects including the flat and out-of-round wheels have been tested and the results validated the fusion method by providing informative patterns.

1. INTRODUCTION

Railway wheels are critical components and detecting their defects is important from safety, maintenance, and operation perspectives. Therefore, several condition monitoring systems have been developed to detect the defective wheels (Alemi, Corman, & Lodewijks, 2017). Wheel Impact Load Detector (WILD) is a condition monitoring system introduced in 1983 to measure high impact forces generated by defective wheels (Partington, 1993). This system exploits the rail vibration (Belotti, Crenna, Michelini, & Rossi, 2006) or the rail strain (Stratman, Liu, & Mahadevan, 2007) to estimate the wheel-rail contact force.

Since the sensors have a limited effective zone, multiple sensors are normally used to sample from the whole wheel circumference. Partington proposed two methods to analyse the data collected by the multiple sensors (Partington, 1993). These methods use the peak force and the average force measured by the sensors. The first method is the ratio of the peak force to the average force that is called the force ratio, and the second method is the subtraction of the peak force and the average force that is called the dynamic force. These values provide bit of information about the wheel out-of-roundness. In addition, the wheel velocity and axle load influence these values (Johansson & Nielsen, 2003). Moreover, using these values to identify the defect type is challenging. Therefore a new method has been proposed to process the data collected by WILD to provide detailed information about the wheel defects (Alemi, Corman, Pang, & Lodewijks, 2017).

The wheel movement over the rail generates a periodic wheel-rail contact force signal. The multiple sensors are sampling from the periodic contact force signal in different locations. Since the location of the sensors and the wheel diameter are the known values, the collected samples can be mapped over the circumferential coordinate to generate a pattern in the space domain. This pattern has a correlation with the wheel geometry, and the contact force. Therefore, the reconstructed patterns can be attributed to the wheel defect to identify the defect type and estimate its severity. This process was already validated using the data simulated by VI-Rail (Alemi, Pang,

Corman, & Lodewijks, 2017), but experimental validation of the multi-sensor data fusion model has been a gap.

This paper aims to validate the data fusion model using the data generated by a laboratory test. Due to the lack of experimental facility, a new test rig has been designed and constructed to model the wheel-rail interaction and to generate the real data required for the fusion model. This paper explains the structure of the new test rig. In this test rig, a rotating arm moves a wheel over a circular rail that is supported by 24 sleepers. According to this symmetric configuration, six strain sensors have been mounted under the rail with constant intervals to measure the rail bending strain. The strain sensors measure different portions of the wheel in discrete points. Therefore, the signals acquired from this measurement presents fragments of information. The fusion model reconstructs patterns from the data collected by the multiple strain sensors for different wheel defects. By reconstructing the informative patterns correlated to the wheel defects, the fusion model is validated.

The paper is structured as follows. Since the detailed explanation of the fusion method has been presented in (Alemi, Corman, Pang, & Lodewijks, 2017), the second section only presents an overview on the data fusion model. Section 3 describes the new test rig and marks the test conditions. Section 4 presents the outputs of the tests and discusses the results obtained from the fusion model using the real data generated by the experimental tests. Finally, section 5 draws the main conclusions.

2. DATA FUSION MODEL

Rail is usually supported by sleepers to transfer the load to the ground. The track structure limits the potential locations for installing the sensors, because the sensors should be installed in the symmetric configuration to give the comparable outputs. Figure 1 presents the schematic view of the rail, and the configuration of the sleepers and sensors. In this figure, the sensors were installed under the rail in the middle point between two consecutive sleepers to measure the rail bending strain. The locations of the sensors are known as a distance vector (X) that is defined with respect to the location of the first sensor.

The wheel is moving over the sensors and each sensor samples from a portion of the wheel. When the wheel is far from the sensor, the output of the sensor is zero. By closing the wheel to the sensor, the output of the sensor increases to a maximum and then decreases to zero. That maximum is called the effective zone and a limited number of samples can be selected from that area. Two sampling methods were developed in the prior research, the Single Sampling Method (SSM) and the Multiple Sampling Method (MSM). Using the MSM more than one sample can be selected from each sensor. When M sensors collect N samples on the effective

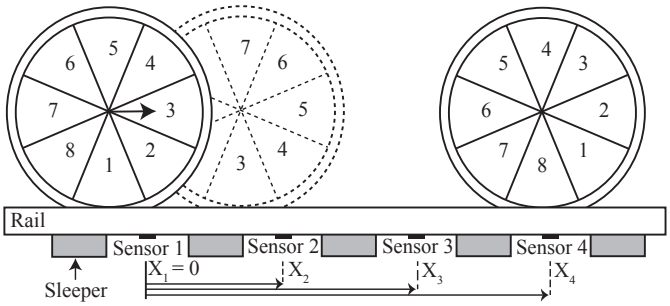

Figure 1. The schematic view of the rail, sleepers and sensors

zone, a dataset from the samples is generated as follows:

$$S_{m,n} = \begin{pmatrix} s_{1,1} & s_{1,2} & \cdots & s_{1,N-1} & s_{1,N} \\ s_{2,1} & s_{2,2} & \cdots & s_{2,N-1} & s_{2,N} \\ \vdots & \vdots & \ddots & \vdots & \vdots \\ s_{M-1,1} & s_{M-1,2} & \cdots & s_{M-1,N-1} & s_{M-1,N} \\ s_{M,1} & s_{M,2} & \cdots & s_{M,N-1} & s_{M,N} \end{pmatrix} \quad (1)$$

This dataset is the magnitude of the samples collected by multiple sensors. Each row presents the samples of a sensor. The sample $s_{1,1}$ is the first samples collected from the wheel by the first sensors. The sample $s_{2,1}$ is the first samples collected from the wheel by the second sensors. The space distance between the sample $s_{1,1}$ and $s_{2,1}$ is equal the sensor distance that is a known value. Since the wheel circumference is a known value, the data collected by the sensors can be mapped over the circumferential coordinate using the following equation:

$$Y_{m,1} = X_m - (L_w \times \lfloor \frac{X_m}{L_w} \rfloor) \quad (2)$$

In this equation, X_m is the sensor position vector, L_w is the wheel circumference, $\lfloor\ \rfloor$ is the round operator toward the nearest integer less than or equal to the element, and $Y_{m,1}$ is the position vector of the data over the circumferential coordinate. The portion of the wheel that is sensed by each sensor is determined using Eq. 2. The remainder after division of the sensor position by the wheel circumference length determines the sample position over the circumferential coordinate. Eq. 2 uses the first column of dataset 1 and maps them over the circumferential coordinate. For mapping the other samples of the dataset, Eq. 2 can be extended to the following equation:

$$Y_{m,n} = Y_{m,1} + ((n-1) \times \lambda) \quad (3)$$

in which $Y_{m,1}$ is the positions of the first sample of each sensor and λ is space interval between the samples that is defined as follows:

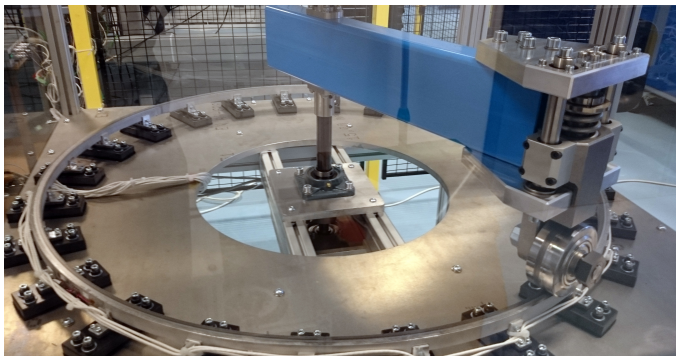

Figure 2. The test rig constructed to generate real data from the wheel-rail interaction

$$\lambda = \frac{V}{f_t} \tag{4}$$

In this equation, V is the wheel velocity and f_t is the sampling frequency of the sensors in the time domain. To see more detailed explanation of the fusion method refer (Alemi, Corman, Pang, & Lodewijks, 2017).

3. TEST RIG

The fusion model combines the samples collected by multiple sensors to generate a new signal. To validate this model, the data simulated by VI-Rail used and the informative patterns were reconstructed (Alemi, Pang, et al., 2017). This paper validates the fusion model using the real data generated in laboratory. To achieve this purpose, a new test rig has been designed and constructed to generate real data as the input of the data fusion model by modelling the wheel-rail interaction.

Figure 2 shows the test rig consisting of a rail, rotating arm, wheel, motor, sleepers, clamps, rubbers, wheel hub, and spring. The circular aluminium rail was connected by clamps to 24 PVC plate as the sleepers that supports the wheel load. One side of the rotating arm was connected to a motor through a shaft and the other side had the wheel hub to hold the wheel. The load of the wheel on the track is adjustable using a spring connected to the wheel hub.

Six strain sensors were installed in the symmetric positions with 60° intervals. The rail was polished and the sensors were glued to the rail. These sensors measured the rail bending strain generated by the wheel-rail contact force. Figure 3 presents the schematic top view of the sensors positions, wheel, rail, sleepers and rotating arm.

The rail had a rectangular profile with 20mm height and 15mm width. The rail diameter is 1007.5mm (central contact point between the wheel and rail) and the wheel diameter is 100mm. According to Eq. 2 and 3, the positions of the sensors (X_n) and the wheel circumference (L_w) are required for fusing the collected data. On each rotation of the arm over the rail, six

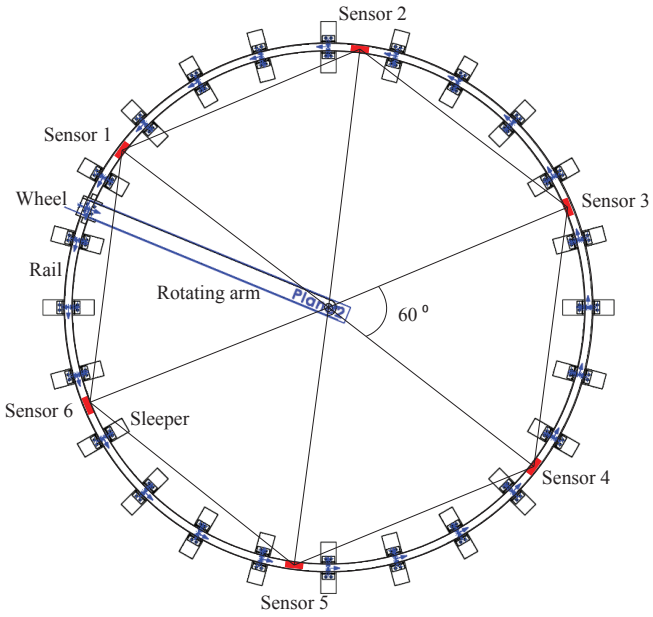

Figure 3. The configuration of six sensors installed under the rail

sensors sample from the wheel. For sampling with more sensors, the arm should have more rotations. This process can be continued to the extent that whole wheel circumference be sampled.

The strain sensors measure the rail bending signal as the response of the rail to the wheel-rail contact force. The rail response is influenced by the wheel load and velocity. Therefore, during each measurement, the wheel load and velocity were kept constant.

To investigate the fusion model, three wheels were tested including a healthy wheel and two other wheels with flat and out-of-round (OOR) defects. The flat wheel had 99.01mm diameter and 0.11mm flat depth. The third order OOR wheel had 98.92mm diameter and 0.08mm amplitude. Next section presents the results of the fusion model using the data generated by the test rig.

4. RESULTS AND DISCUSSION

The sensors were connected through an amplifier to the computer. The output of the sensors was the voltage variation over time. Normally the measured voltage signal is converted to the strain signal and then using a known force is converted to the force signal. Since the output of the data fusion model is a pattern, the sensor output in the voltage was directly used for further processing without converting to the strain or force. Figure 4 presents the output of a sensor during the passage of the healthy wheel. In this signal, the output of the sensor is zero when the wheel is far from the sensor. By approaching the wheel to the sensor, the output of the sensor changed.

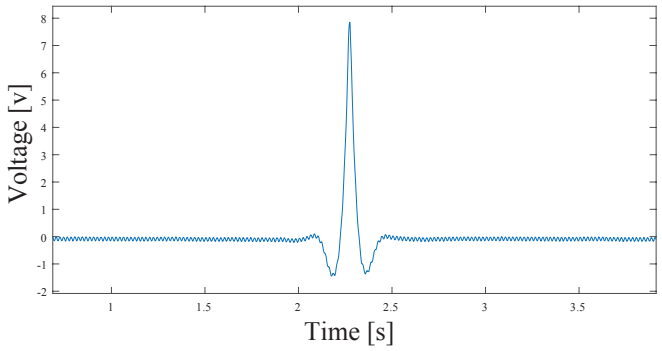

Figure 4. The output of a strain sensor during the passage of the healthy wheel

When the wheel is close to the sensor in a way that is not on top of the sensor, the rail goes up and compresses the sensor and provides negative output. When the wheel passes the sensor, the output of the sensor increases to a maximum that depends on the wheel-rail contact force. This signal depends on the dynamic parameters of the test rig but it is generally comparable to the signal measured from the field tests (Filograno, Corredera, Rodriguez-Plaza, Andres-Alguacil, & Gonzalez-Herraez, 2013).

According to Figure 3, the sensors were configured with a constant distance. When the wheel is healthy and moving with constant velocity, the sensors provide similar outputs with a constant delay. Figure 5 presents the outputs of the six sensors in the first round of the healthy wheel rotation over the sensors. Each sensor measures a portion of the wheel. The magnitude of the peaks in the signals measured by each sensor depends on the wheel-rail contact force and basically on the wheel portion that contacts with rail. When the wheel is healthy, the sensors measure signals with similar magnitude in the peaks.

In this circular test rig, more rotations of the wheel is equal the extension of the number of sensors. On each rotation, 6 sensors sample from the wheel. Therefore, 10 rotations of the wheel lead to sampling with 60 sensors. Figure 6 presents the outputs of 60 sensors for the healthy wheel. In this Figure, the sensors provided similar outputs with small variations.

By selecting few samples from the peak on each sensor, a dataset like presented in Eq. 1 can be generated. Figure 7 compares the samples measured by 60 sensors after selecting 11 samples per sensor using the MSM for the healthy, flat, and OOR wheels. In Figure 7(a) that the wheel is healthy, the samples have very small deviation from their average. In Figure 7(b) and (c) that correspond to the flat, and OOR wheels, the samples have a considerable deviation from their average. This deviation acknowledges the existence of the wheel defects but fails in providing detailed insight about the wheel defects.

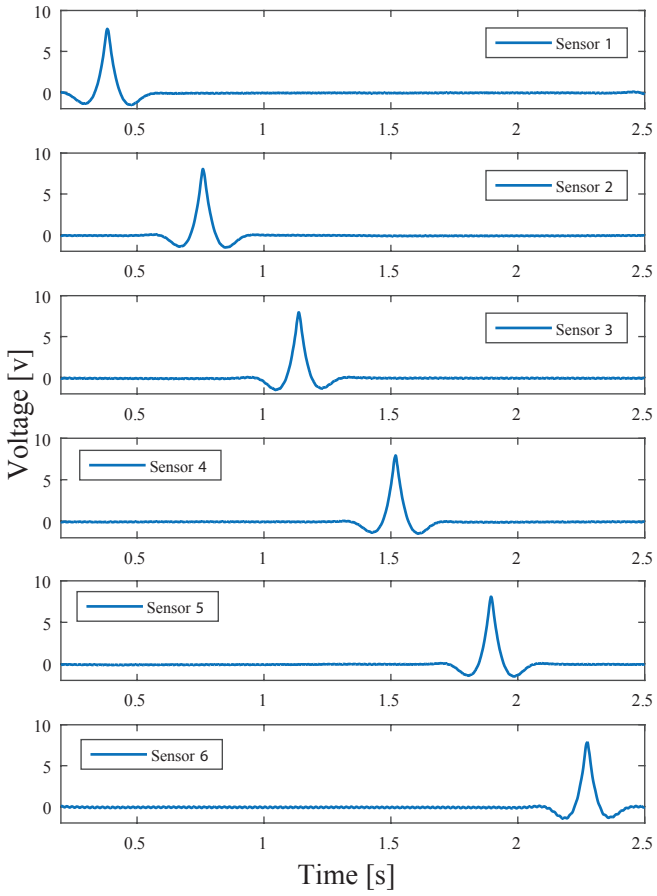

Figure 5. The outputs of the strain sensors during the first passage of the wheel

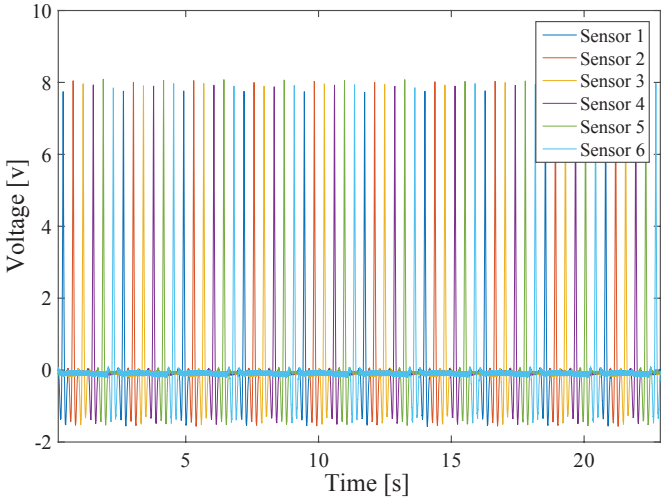

Figure 6. The outputs of the 60 sensors for the healthy wheel

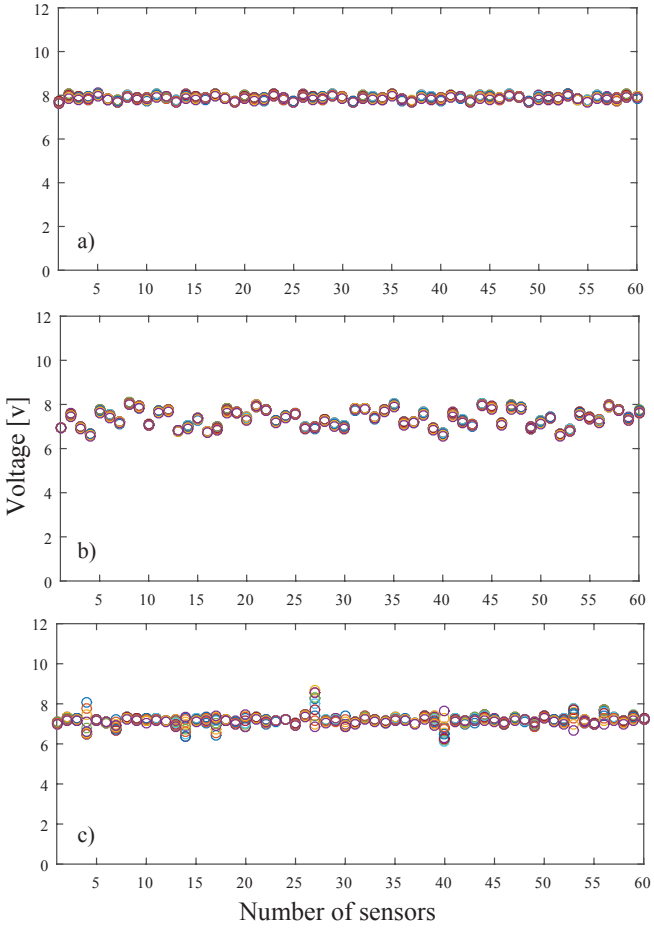

Figure 7. The comparison between the samples selected from 60 sensors for a) the healthy wheel. b) the OOR wheel, and c) the flat wheel

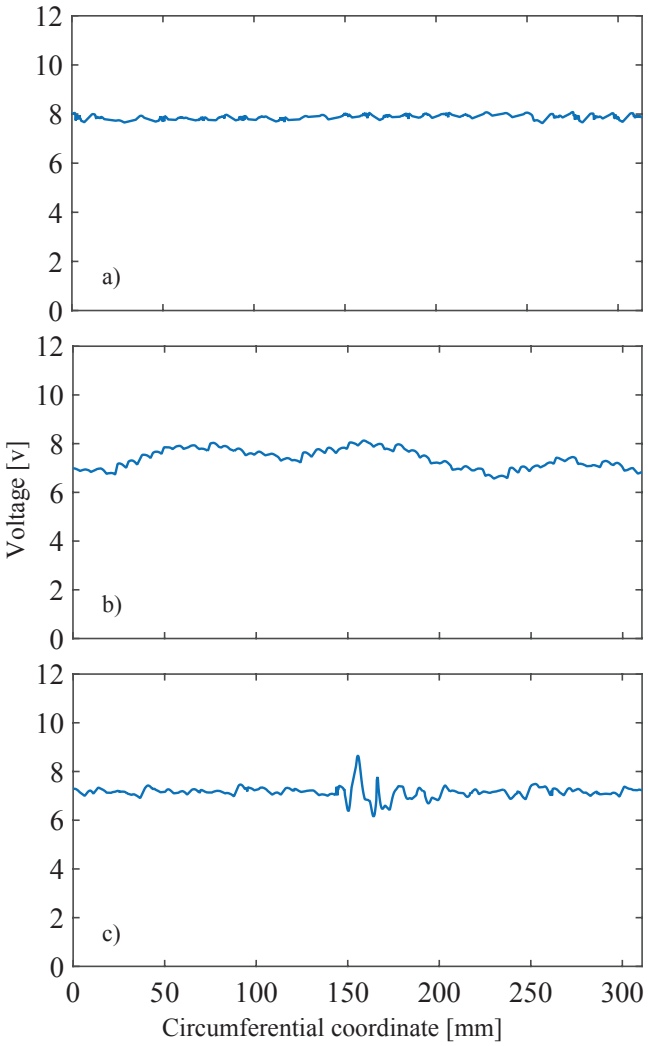

Figure 8. The comparison between the patterns reconstructed using the samples collected from 60 sensors for a) the healthy wheel. b) the OOR wheel, and c) the flat wheel

Using the Eq. (1-3) the selected samples presented in Figure 7, have been fused and mapped over the circumferential coordinate to generate a pattern. Figure 8 compares the results of the fusion model for three wheels. In this Figure, the length of the signals equals to the wheel circumference. Figure 8(a) shows a flat pattern corresponding to the healthy wheel. Figure 8(b) displays a sinusoidal pattern corresponding to the 3rd order out of round wheel. Figure 8(c) demonstrates a pattern containing a peak corresponding to the flat.

The comparison between the patterns reconstructed in Figure 8 clearly shows the nature of the defects generated the wheel-rail contact force. These results perfectly validate the fusion model and the possibility of generating informative signals from the samples collected by WILD.

5. CONCLUSION

Wheel defect Identification is a vital task and a common method for detecting the sever wheel defect is measuring the wheel load using Wheel Impact Load Detectors. Since WILDs measure the wheel force in discrete points, a fusion method has been proposed to reconstruct a pattern from the samples collected by WILDs. This research validated the fusion method using the data collected in the laboratory. A test rig has been built and three wheels have been used to generate the required data. The patterns reconstructed by the fusion method demonstrated a considerable similarity with the wheel defects. Therefore, the reconstructed signals can be used in the further research for identifying the defect type and severity.

ACKNOWLEDGMENT

The authors would like to acknowledge Ed Stok and Freek Brakel for giving the technical supports and Perry Posthoorn for building the test rig.

REFERENCES

Alemi, A., Corman, F., & Lodewijks, G. (2017, sep). Condition monitoring approaches for the detection of railway wheel defects. *Proceedings of the Institution of Mechanical Engineers, Part F: Journal of Rail and Rapid Transit*, *231*(8), 961–981. doi: 10.1177/0954409716656218

Alemi, A., Corman, F., Pang, Y., & Lodewijks, G. (2017). Reconstruction of railway wheel defect signal from wheel-rail contact signals measured by multiple wayside sensors. *Proceedings of the Institution of Mechanical Engineers, Part F: Journal of Rail and Rapid Transit*(X), 1–10.

Alemi, A., Pang, Y., Corman, F., & Lodewijks, G. (2017). Railway Wheel Defect Identification Using the Signals Reconstructed from Impact Load Data. In F.-K. Chang & F. Kopsaftopoulos (Eds.), *11th international workshop on structural health monitoring* (pp. 1511–1518). Stanford.

Belotti, V., Crenna, F., Michelini, R. C., & Rossi, G. B. (2006, nov). Wheel-flat diagnostic tool via wavelet transform. *Mechanical Systems and Signal Processing*, *20*(8), 1953–1966. doi: 10.1016/j.ymssp.2005.12.012

Filograno, M. L., Corredera, P., Rodriguez-Plaza, M., Andres-Alguacil, A., & Gonzalez-Herraez, M. (2013, dec). Wheel Flat Detection in High-Speed Railway Systems Using Fiber Bragg Gratings. *IEEE Sensors Journal*, *13*(12), 4808–4816. doi: 10.1109/JSEN.2013.2274008

Johansson, A., & Nielsen, J. O. (2003, jan). Out-of-round railway wheels - wheel-rail contact forces and track response derived from field tests and numerical simulations. *Proceedings of the Institution of Mechanical Engineers, Part F: Journal of Rail and Rapid Transit*, *217*(2), 135–146. doi: 10.1243/095440903765762878

Partington, W. (1993, jan). Wheel impact load monitoring. *Proceedings of the ICE - Transport*, *100*(4), 243–245. doi: 10.1680/itran.1993.25451

Stratman, B., Liu, Y., & Mahadevan, S. (2007, jul). Structural health monitoring of railroad wheels using wheel impact load detectors. *Journal of Failure Analysis and Prevention*, *7*(3), 218–225. doi: 10.1007/s11668-007-9043-3